Available online at www.sciencedirect.com
SCIENCE DIRECT®
Pergamon
Acta Materialia 51 (2003) 347–364
Acta MATERIALIA
www.actamat-journals.com

Dependence of intergranular fatigue cracking on the interactions of persistent slip bands with grain boundaries

Z.F. Zhang [ab,*], Z.G. Wang [a]

[a] *Division for Materials Fatigue, Shenyang National Laboratory for Materials Science, Institute of Metal Research, Chinese Academy of Sciences, Shenyang, 110016, China*
[b] *IFW-Dresden, Institute for Metallic Materials, P.O. Box 27 00 16, D-01171, Dresden, Germany*

Received 9 May 2002; received in revised form 23 July 2002; accepted 30 August 2002

Abstract

Intergranular fatigue cracking mechanisms in various copper crystals with different grain boundaries (GBs) were systematically investigated and summarized. In the present investigation, the GBs are classified into three types, i.e. (I) random large-angle GBs parallel, perpendicular or tilting to the stress axis in various copper bicrystals; (II) low-angle GBs parallel or perpendicular to the stress axis in copper columnar crystals; (III) large-angle Σ19b GB in a special $[\bar{4}1520]/[18\bar{2}7]$copper bicrystal. The slip planes of the adjacent crystals are coplanar across the later two types of GBs, but the slip directions of the two component grains are different beside the Σ19b GB. With the help of electron channeling contrast (ECC) technique in scanning electron microscopy (SEM), fatigue cracks and the interactions of dislocations with the GBs in all the fatigued crystals were observed and revealed. The results show that all the large-angle GBs (type I) in copper bicrystals always become the preferential sites to initiate fatigue cracks, independent of the interaction angle between the GB plane and the stress axis. This intergranular fatigue cracking mechanism can be attributed to the piling-up of dislocations at the large-angle GBs. For the columnar crystals containing low-angle GBs (type II), it is observed that persistent slip bands (PSBs), which transfer through low-angle GBs continuously, are the preferential sites for the nucleation of fatigue cracks. However, fatigue cracks were never observed at the low-angle GBs, no matter whether they were perpendicular or parallel to the stress axis. The non-cracking behavior of the low-angle GBs can be explained by the continuity of the dislocations, which led to the disappearance of piling-up of dislocations. For the Σ19b GB (type III), it is found that the favorable fatigue cracking mechanism is still intergranular type in comparison with PSB cracking even though the two component grains have a coplanar slip system. The corresponding GB cracking mechanism should be attributed to the difference in the slip directions between two component grains, which only allows for partial passing through of dislocations across the Σ19b GB. Based on the results above, it is suggested that intergranular fatigue cracking strongly depends on the interactions of PSBs with GBs in fatigued crystals, rather than the GB structure itself. Among all the GBs, only the low-angle GBs are intrinsically strong to resist the nucleation of fatigue cracks under cyclic loading.

Keywords: Copper bicrystals; Grain boundaries (GBs); Fatigue cracking; Persistent slip bands (PSBs)

1359-6454/03/$30.00 © 2002 Acta Materialia Inc. Published by Elsevier Science Ltd. All rights reserved.
doi:10.1016/S1359-6454(02)00399-3

1. Introduction

Nano-crystalline materials have been attracting rapidly increasing interest in recent years and have the potential of revolutionizing traditional materials due to their excellent properties [1–4]. With decreasing grain sizes, the volume fraction of grain boundaries (GBs) will be increased significantly, accordingly, GBs play a more and more important role in the properties of the aggregates. On one hand, grain refinement will improve the strength of materials due to the blocking dislocations of GBs. On the other hand, GBs are often the potential sites for the nucleation of cracks, even serving as fracture path in polycrystals. So far both beneficial and detrimental effects of GBs on the properties of polycrystals coexist. Therefore, the phenomena associated with GBs have been given much more attention by many researchers [5–8]. For a better understanding of the effect of GBs on the damage behavior of polycrystalline materials, the concepts of GB character distribution (GBCD) and GB engineering (GBE) have been proposed to predict the properties of materials through considering some special GBs, which are insensitive to nucleation of cracks under external stress or in an aggressive environment [9–13]. Therefore, a question then arises: *what types of GBs are those special ones*? To solve the question, nowadays, some factors have been considered for the special GBs [8–14]: (a) GB misorientation angle $\Delta\theta$; (b) coincidence site lattice boundaries (CSL); (c) misorientation and GB plane geometry; (d) interface damage function. It is originally thought that any CSL boundary with a low Σ value generally has some special properties. However, the principle drawback of the CSL model is that only the orientation relationship between adjacent grains is specified rather than the relationship actually at the boundary surface itself. On the other hand, GB misorientation angle $\Delta\theta$ is considered as the simplest description of the GB structure. According to the value of $\Delta\theta$, GBs are classified into high-angle ($> 15°$) and low-angle type ($< 15°$). It is noted that the high-angle GBs are always more sensitive to cracking than the low-angle GBs [8].

Although some factors can explain the cracking behavior of polycrystalline materials, however, the situation under fatigue loading seems to be more complicated than that under the uniaxial loading. It is well known that GBs are often regarded as the strengthening elements in comparison with the interior of grains in ductile polycrystals. However, it is often observed that persistent slip bands (PSBs) are often activated and GBs become the obstacle to propagation of slip bands during cyclic deformation of polycrystalline Cu and Ni [15,16]. Therefore, the interactions or interaction modes of slip bands with different GBs will affect intergranular fatigue cracking processes. Unfortunately, up to date, there are no systematical investigations and reports concerning intergranular fatigue cracking induced by the interactions of slip bands with GBs. Since GBs often block the propagation of slip bands, regardless of the GB structure, we may classify all the GBs into three types. (I) Random large-angle GBs; the GBs can make an arbitrary angle with respect to the stress axis and the slip planes of the adjacent grains are not coplanar. Therefore, this type of GBs can be regarded as the obstacles to slip bands under plastic deformation. (II) Low-angle GBs with small misorientation; the GBs can also make any angle with respect to the stress axis. But all the slip planes of the neighboring grains are coplanar and the slip directions of the two coplanar slip systems are nearly the same due to small misorientation. The special crystallographic relations will allow for the passing through of slip bands across low-angle GBs. (III) Some special GB; there is one group of coplanar slip systems between the component crystals, but the slip directions of the two grains are obviously different. Therefore, we will emphasize the interactions of slip bands with the three types of GBs and the consequent fatigue cracking behavior, which is quite different from the GBCD model [9–13]. In addition, we note that electron channeling contrast (ECC) technique in scanning electron microscopy (SEM) has been widely applied to observe the dislocations in deformed materials [16–20]. In comparison with the traditional TEM technique, the

* Corresponding author. Tel.: 0049 351 4659766; fax: 0049 351 4659541.
E-mail address: z.f.zhang@ifw-dresden.de (Z.F. Zhang).

advantages of the SEM-ECC technique are the simple specimen preparation and the possibility of studying wide areas on the same specimen. In particular, it is convenient to observe the dislocation arrangements at some special sites, such as near the GBs [21,22], deformation bands [23,24] and cracks [22,24–26]. For the fatigued specimens, therefore, it is readily to reveal the evolution of dislocations on a large area and at some special sites, such as the interactions of PSBs with GBs during cyclic deformation. Furthermore, micromechanism of fatigue cracking can be well revealed and understood. In this paper, we will reveal and summarize the dependence of intergranular fatigue cracking on the interactions of PSBs with the three types of GBs in copper crystals through the SEM-ECC technique.

2. Experimental procedure

To clarify fatigue damage mechanisms of all types of GBs, some bulk of bicrystal plates were grown from the OFHC copper of 99.999% purity by the Bridgman method in a horizontal furnace. The growth processes of the bicrystals can be illustrated as in Fig. 1(a). At one side of a graphite mold, two seed grains (G1 and G2) with different orientations were put into the grooves. Then the graphite mold was placed into some pure copper for growth. After that, the graphite mold containing two seed grains and pure copper was put into a horizontal furnace. Before heating, the furnace was evacuated to a pressure of 10^{-3} Pa. Then, the furnace was heated in an Ar atmosphere and the temperature in the graphite mold was controlled to be 1200 °C, which is higher than the melting point (1080 °C) of pure copper. At the side of seed grains, the temperature was controlled to be lower than the melting point of copper through enwinding a water-cooling copper tube. Under suitable conditions, the two seed grains will not melt and can make contact with the liquid copper in the mold. With moving the mold from right to left, the two seed grains will gradually grow up and a GB can form in the middle of the mold under the controlled conditions. In the end, the bicrystal can grow to the dimension of 200 mm×50 mm×15 mm, as shown in Fig. 1(b), therefore, several types of fatigue specimens with a GB plane perpendicular, tilting or parallel to the stress axis can be cut from the bulk bicrystal plates.

Fig. 2(a) shows a typical fatigue specimen of copper bicrystals containing a perpendicular large-angle GB, including $[\bar{1}23]\perp[335]$, $[\bar{5}913]\perp[\bar{5}79]$ and $[014]\perp[\bar{1}15]$ copper bicrystals [27–30]. Fig. 2(b) gives the schematic diagram of the copper

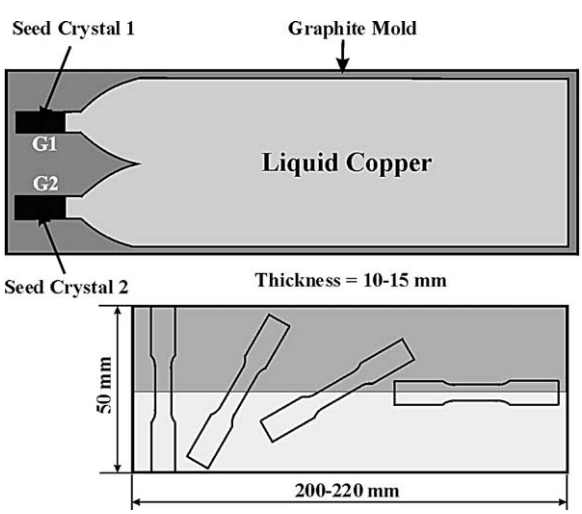

Fig. 1. (a) Illustration of a copper bicrystal with two different seed grains G1 and G2 grown in a horizontal furnace; (b) The as-grown bulk copper bicrystal plate and the bicrystal specimens with different GB.

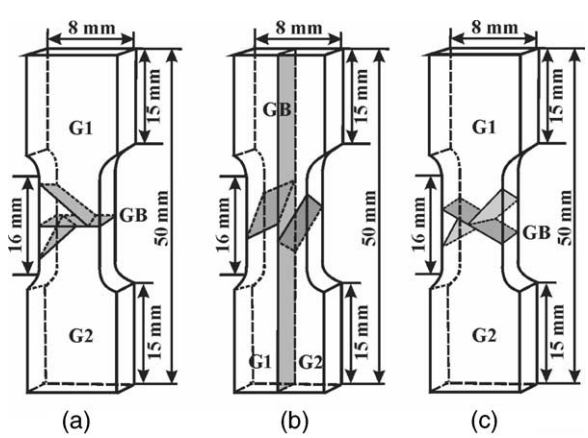

Fig. 2. Illustration of fatigue specimens and crystallographic relationships of the copper bicrystals with a large-angle GB perpendicular, parallel or tilting to the stress axis.

bicrystals with a parallel large-angle GB, including [$\bar{6}$79]//[$\bar{1}$45], [$\bar{3}$610]//[$\bar{4}$57] and [$\bar{4}$916]//[$\bar{4}$927] copper bicrystals [31–33]. Besides, some bicrystal specimens with a GB tilting to the stress axis were also prepared, as shown in Fig. 2(c) [34]. In those bicrystals, the GBs are typical random large-angle one and are defined as type I GB in the present investigation. One of the common crystallographic features in those copper bicrystals is that there is no coplanar slip system between the neighboring grains, as illustrated in Fig. 2(a–c). In addition, some columnar copper crystal specimens containing several low-angle GBs basically parallel or perpendicular to the stress axis were also grown and prepared, as shown in Fig. 3(a) and (b). The average axis orientations of the two groups of columnar crystal specimens are typical single slip, as respectively marked in the standard stereographic triangle in Fig. 3(c). The misorientations between the adjacent grains were measured to be in the range of 3–5° [35,36]. The GBs in the columnar crystals are defined as type II GB, and all the slip systems of the adjacent grains will be coplanar. Fig. 4(a) and (b) show a special [$\bar{4}$1520]/[18$\bar{2}$7] copper bicrystal specimen, in which two component grains have a common primary slip plane and a GB inclines to the stress axis [37]. By electron back-scattering-diffraction (EBSD) technique, it is found that the rotation angle of the two component grains is 46.2° around the common rotation [111] axes. Therefore, the GB

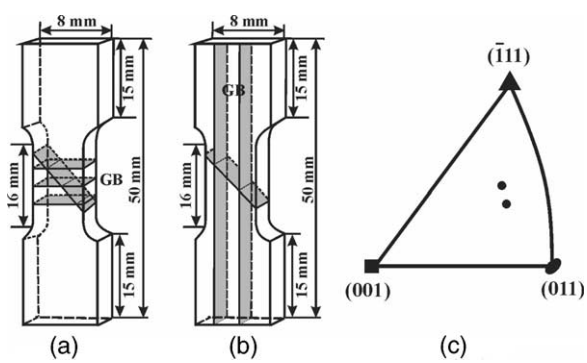

Fig. 3. (a) and (b) Illustration of fatigue specimens and crystallographic relationships of the copper columnar crystals with GBs perpendicular or parallel to the stress axis. (c) The average orientations of the columnar crystals in the standard stereographic triangle.

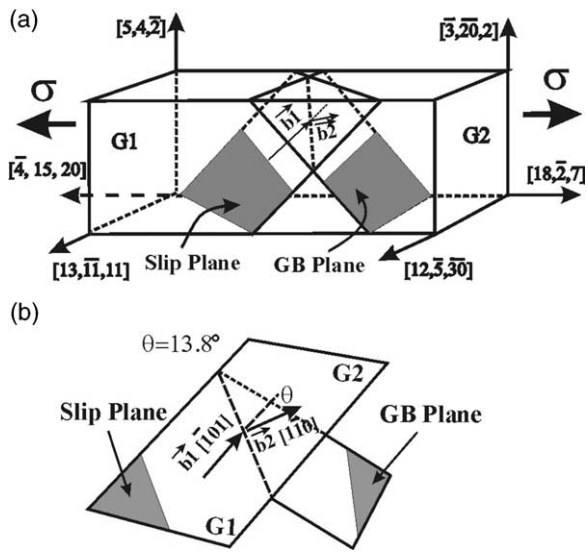

Fig. 4. (a) Crystallographic relationships of the [$\bar{4}$1520]/[18$\bar{2}$7] copper bicrystal with common primary slip plane and a Σ19b GB tilting to the stress axis. (b) Interaction of the common slip plane with the GB plane.

is a CSL Σ19b GB in type and the angle between the slip directions of the two component crystals is equal to 13.8° under the present stress condition. The Σ19b GB in the [$\bar{4}$1520]/[18$\bar{2}$7] bicrystal is defined as type III GB and is also a large-angle type. The community between the type II and III GBs is that the component grains beside the GBs have a coplanar slip system, but the slip directions of the coplanar slip systems are different in the special [$\bar{4}$1520]/[18$\bar{2}$7] bicrystal, as illustrated in Fig. 4.

Before fatigue testing, the specimens were electrolytically polished to produce a strain-free surface for microscopic observation. All the specimens were cyclically deformed in push–pull on a Shimadzu servo-hydraulic testing machine under constant plastic strain control at room temperature in air. Cyclic deformation was interrupted at different cycles, then the surfaces of those specimens were observed in a Cambridge S360 SEM to examine slip morphology and fatigue cracks. In addition, the SEM-ECC technique was employed to investigate the interactions of PSBs with different types of GBs during cyclic deformation, as reported in the literature [16–20]. To compare with

the dislocation patterns observed by TEM technique, an inverted imaging mode is adopted in the present investigation. Accordingly, the bright areas in the ECC micrograph will represent the dislocation-poor regions, whereas the dark areas should correspond to the dislocation-dense regions.

3. Experimental results

3.1. Fatigue cracking behavior in bicrystals containing type I GBs

During cyclic deformation, $[\bar{1}23]\perp[\bar{3}35]$, $[\bar{5}913]\perp[\bar{5}79]$ and $[014]\perp[\bar{1}15]$ copper bicrystals with a perpendicular GB exhibit rapid initial cyclic hardening and consequent cyclic saturation behavior [27–30]. Surface observations reveal that many PSBs are activated on the two component grains of the bicrystals, however, all the PSBs terminate at the GBs. Fig. 5(a) and (b) show typical interactions of slip bands with a perpendicular GB in those bicrystals. In general, primary slip bands can transfer through the whole component grains and sometimes some secondary slip bands occur near the GBs, depending on the orientations of the component grains. If cyclic deformation continues to apply on the specimens, after a long cyclic saturation, a rapid cyclic softening corresponding to fatigue crack initiation can be found. Surface observations show that all the fatigue cracks nucleate and propagate along the GB in all the copper bicrystals above. Fig. 6(a) shows a typical intergranular fatigue cracking of the bicrystals with a perpendicular GB. It is noted that there are only primary slip bands near the GB even the intergranular crack has opened a larger displacement (about 40 μm). It seems that primary slip bands should control the GB fatigue cracking process of the bicrystals. With further cyclic deformation, fatigue crack will continue to propagate along the GB gradually, until the occurrence of intergranular fatigue fracture. If the observations are focused on

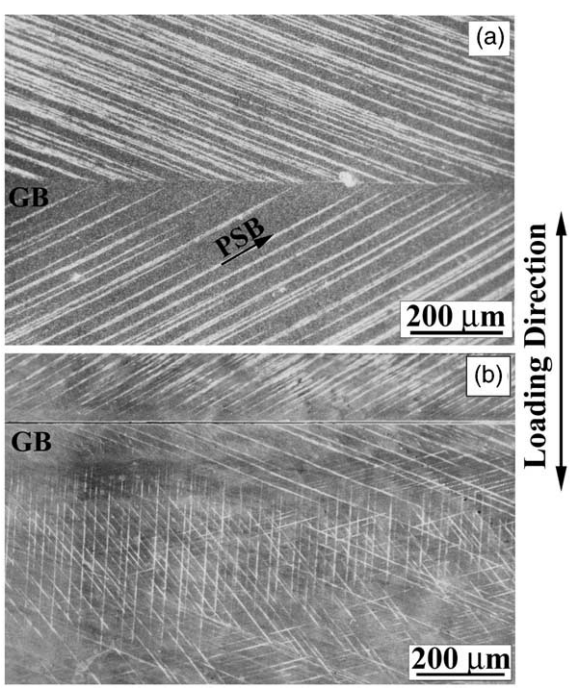

Fig. 5. Surface slip morphologies of the copper bicrystals with a perpendicular large-angle GB. (a) $[\bar{5}913]\perp[\bar{5}79]$ copper bicrystal. The activated slip systems of the two grains are $(111)[\bar{1}01]$; (b) $[\bar{1}23]\perp[\bar{3}35]$ copper bicrystal. The activated slip system for the upper $[\bar{1}23]$ grain is $(111)[\bar{1}01]$, the lower $[\bar{1}23]$ grain is $(111)[\bar{1}01]$ and $(111)[011]$.

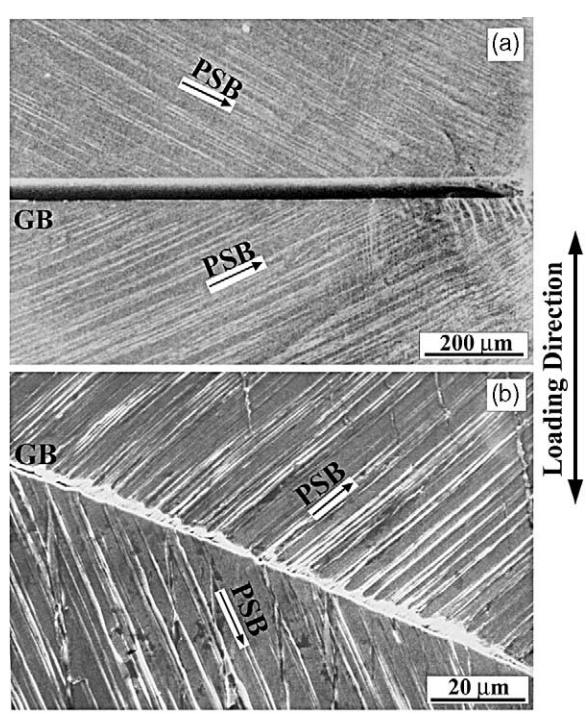

Fig. 6. Intergranular fatigue cracking in the bicrystal with a large-angle perpendicular (a) and tilting to the stress axis (b).

the whole surface of the bicrystals, however, PSBs never become the sites of fatigue cracking after intergranular fracture of the bicrystals. These results are consistent with the observations in $[\bar{1}17]\perp[\bar{3}45]$, $[\bar{1}34]\perp[\bar{1}34]$, $[001]\perp[\bar{1}49]$ and $[\bar{1}49]\perp[\bar{1}49]$ copper bicrystals by Hu and Wang [38,39], Peralta and Laird [40,41]. In those copper bicrystals, the secondary slip bands were activated near the GBs due to double- or multi-slip orientations of the component crystals. Besides, Hashimoto et al. [42], and Shoji et al. [43] investigated the fatigue cracking behavior of the bicrystals with a perpendicular GB, they also found that fatigue cracks can nucleate and propagate along the GB during cyclic deformation even though some GBs have a low Σ value, such as $\Sigma3$, $\Sigma9$ and $\Sigma41$ GBs. For the copper bicrystal with a GB tilting to the stress axis, we also find that GB cracking is the unique cracking mode no matter under low or high strain amplitude, as shown in Fig. 6(b), which is identical with the bicrystal with a perpendicular GB. From all the results above, it can be concluded that intergranular fatigue cracking is the dominant damage mode even though the orientations of the component grains and the GB structures are obviously different in the copper bicrystals with a perpendicular or tilting GB during cyclic deformation. In other words, the existence of a GB will significantly decrease the fatigue lives of the bicrystals due to early occurrence of intergranular fatigue cracking [35].

On the other hand, when cyclic deformation are performed on $[\bar{6}79]//[\bar{1}45]$, $[\bar{3}610]//[\bar{4}57]$ and $[\bar{4}916]//[\bar{4}927]$ copper bicrystals with a parallel GB, it is found that strain incompatibility in the vicinity of GB always become more serious in comparison with the bicrystals with a perpendicular GB [31–33]. Fig. 7(a) shows typical deformation morphology near the GB in a fatigued $[\bar{6}79]//[\bar{1}45]$ copper bicrystal. Clearly, secondary slip bands are activated near the GB, but deformation morphology strongly depends on the applied strain amplitude. It had been confirmed that there is always a GB affected zone (GBAZ) induced by plastic strain incompatibility [31–33]. With increasing strain amplitude, the width of GBAZ also increases and the degree of plastic strain incompatibility within the GBAZ become

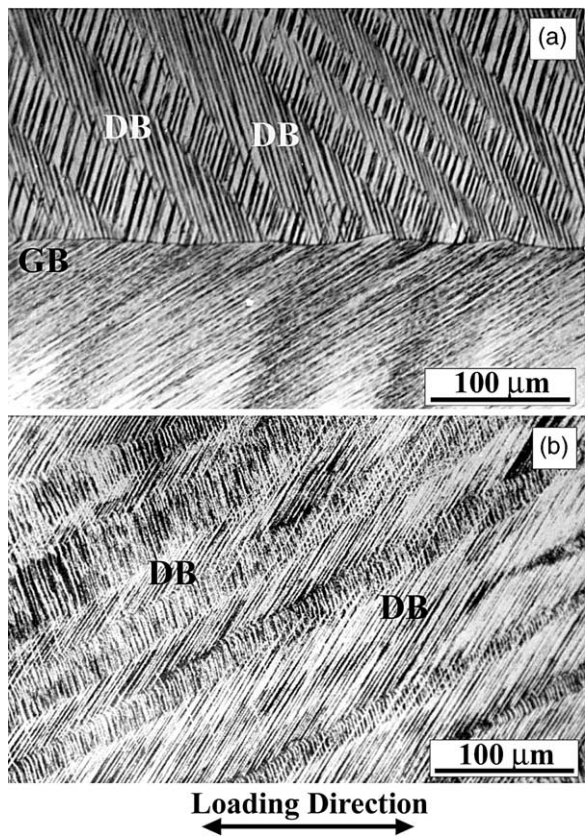

Fig. 7. (a) Slip morphologies beside the GB of the $[\bar{6}79]//[\bar{1}45]$ copper bicrystal. The secondary slip bands and deformation bands (DBs) only occur in the upper $[\bar{1}45]$ grain; (b) Slip morphologies within the GB affected zone in the $[\bar{4}927]$ grain of the $[\bar{4}916]//[\bar{4}927]$ copper bicrystal.

serious, which often leads to GB strengthening effect and disappearance of the plateau in its cyclic stress-strain curve (CSSC). For $[\bar{4}916]//[\bar{4}927]$ copper bicrystal, when it is deformed at low strain amplitude, only secondary slip bands appear near the GB and primary slip bands cannot reach the GB [32]. At higher strain amplitude, both primary and secondary bands can reach the GB and strain incompatibility often become serious, as shown in Fig. 7(b). For $[\bar{1}35]//[\bar{1}35]$, $[\bar{1}35]//[\bar{2}35]$ and $[\bar{2}35]//[\bar{2}35]$ copper bicrystals with a low Σ GB parallel to the stress axis, Hu et al. [44] also observed obvious secondary slip near the GB. The strain incompatibility near the GBs had been widely observed in different bicrystals subjected to unaxial deformation [45–48], however, strain

incompatibility induced by cyclic deformation seems to be more serious and complicated [31–33]. But a common feature near the GB is the appearance of secondary slip bands and the GBAZ.

With continuous cyclic deformation, it is observed that fatigue cracks first nucleate along GB in all the bicrystals above even though the GB is parallel to the stress axis. As an example, fatigue cracking processes of $[\bar{4}916]//[\bar{4}927]$ bicrystal are elucidated and shown in Fig. 8(a)–(c). When the bicrystal is cyclically deformed at low strain amplitude ($\epsilon_{pl} = 5 \times 10^{-4}$), fatigue crack nucleation seems to be rather difficult. After longer cycles (about 5×10^4), some cracks begin to initiate at the intersection sites of PSBs with GB, as shown in Fig. 8(a). With further cyclic deformation, the number of fatigue cracks increases and links each other along the GB, in the end, forming a long intergranular crack. At higher strain amplitude ($\epsilon_{pl} = 2 \times 10^{-3}$), as cyclic number is higher than 10^4, obvious cracks nucleating along GB can be clearly seen (Fig. 8(b)). It can be seen that there is serious strain incompatibility near the GB and both primary and secondary slip bands intersect at the GB. The fatigue crack had propagated to be rather long, finally can extend to the whole gauge region of the bicrystal specimen. In particular, the intergranular cracking path displays a zigzag feature at some region owing to the interactions of PSBs with GB. As cyclic number is high enough ($N > 10^5$), GB cracks become very wide, as shown in Fig. 8(c), a rift with a width of 10 μm can be seen. However, no apparent fatigue cracking along those PSBs is found on the component grain surface except some extrusions on the surfaces. For $[\bar{6}79]//[145]$ and $[\bar{3}610]//[\bar{4}57]$ copper bicrystals, intergranular fatigue cracking processes are nearly the same as $[\bar{4}916]//[\bar{4}927]$ bicrystal. Besides, GB fatigue cracks are also observed to preferentially nucleate in $[\bar{1}35]//[\bar{1}35]$, $[\bar{1}35]//[235]$ and $[\bar{2}35]//[\bar{2}35]$ copper bicrystals with a parallel $\Sigma 3$ or $\Sigma 13a$ GB during cyclic deformation. These results further indicate that large-angle GBs in the bicrystals are preferential sites leading to fatigue cracking even though they are parallel to the stress axis.

From the results above, it can be concluded that the GB cracking was the preferential damage mode

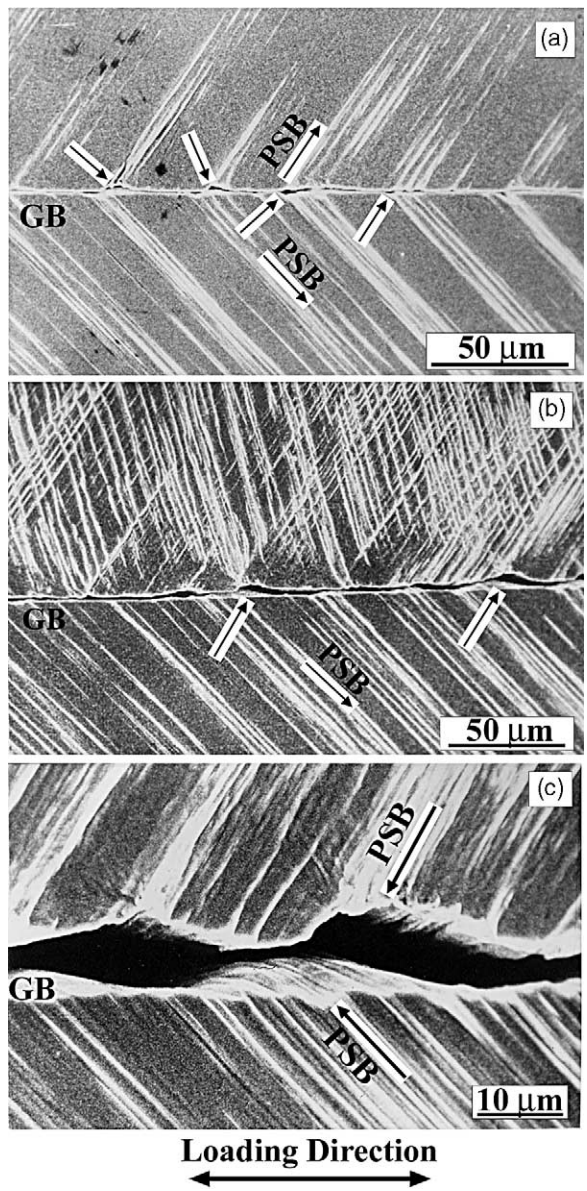

Fig. 8. Fatigue cracking along the GB parallel to the stress axis in the $[\bar{4}916]//[\bar{4}927]$ copper bicrystal deformed at low and high strain amplitudes for different cycles. (a) $\epsilon_{pl} = 5 \times 10^{-4}$, $N = 2 \times 10^5$; (b) $\epsilon_{pl} = 2 \times 10^{-3}$, $N = 2 \times 10^4$; (c) $\epsilon_{pl} = 2 \times 10^{-3}$, $N = 2 \times 10^5$.

in copper bicrystals, no matter whether they are perpendicular, tilting or parallel to the stress axis. In other words, for all the type I GBs in copper bicrystals, the preferential intergranular fatigue cracking behavior is independent of the GB struc-

ture and the interaction angle between the GB plane and the stress axis.

3.2. Fatigue cracking behavior in the crystals containing type II GBs

For the copper columnar crystals containing low-angle GBs, it is found that all the fatigued specimens display initial cyclic hardening and saturation behavior. The cyclic saturation resolved shear stress ranges from 29.0–29.6 MPa in applied strain range of 7×10^{-4} to 4.7×10^{-3} [36], which is similar to that of copper single crystals with single-slip-orientations [49–51]. It indicates that the low-angle GBs do not show a perceivable effect on its cyclic stress–strain response. The result is quite different from that of $[\bar{6}79]//[\bar{1}45]$, $[\bar{3}610]//[\bar{4}57]$ and $[\bar{4}916]//[\bar{4}927]$ bicrystals with a large-angle GB, which often plays an obvious strengthening role in the bicrystals and results in an increase in the saturation stress [31–33]. Surface observations show that all the slip bands beside the low-angle GBs have a good one-to-one relationship, as shown in Fig. 9(a) and (b), indicating that PSBs had transferred trough the low-angle GB continuously. Meanwhile, no secondary slip bands are activated, which further demonstrates good strain compatibility near the low-angle GBs. The transmission of slip bands across low-angle GBs was also observed in deformed titanium by Kehagias et al. [52]. Therefore, the interactions of slip bands with low-angle GBs should be more compatible in comparison with those near large-angle GBs. With further cyclic deformation, it is found that the fatigue cracks are difficult to initiate in the columnar crystals. However, as the cyclic number is high enough, fatigue crack always preferentially nucleates along PSBs, rather than along low-angle GBs, independent of the interaction angle between the GB plane and the stress axis. Fig. 10 shows a typical fatigue crack initiating along PSBs, in the end, leading to transgranular fatigue fracture. With increasing strain amplitude and cyclic number, fatigue cracks invariably nucleate along PSBs, however, intergranular crack is never observed along low-angle GBs during cyclic deformation of the columnar copper crystals. From the present results, it indicates that fatigue crack initiation and fracture along PSBs is the dominant damage mode in columnar copper crystals with low-angle GBs, which is similar to copper single crystals [53–55], but is against with copper bicrystals with large-angle GBs.

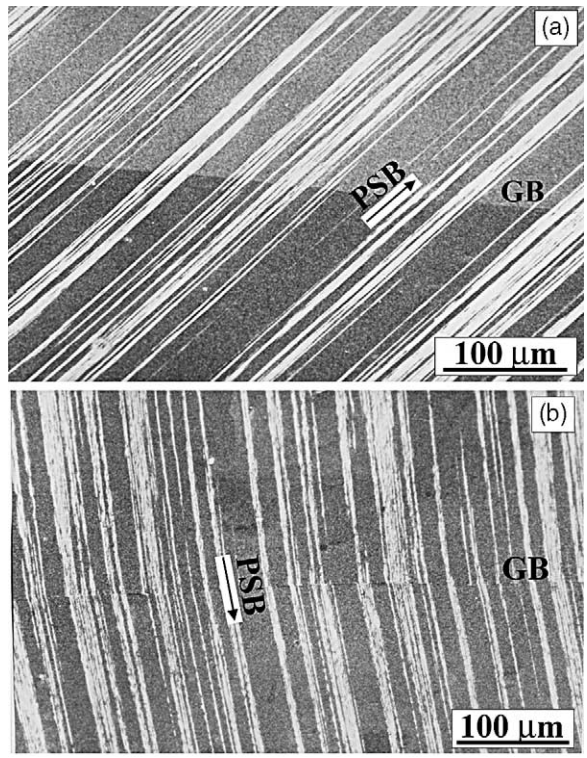

Fig. 9. Surface slip morphologies of the columnar copper crystals containing low-angle GBs. All the slip bands have a good one-to-one relationship across the low-angle GBs, no matter whether they are perpendicular or parallel to the stress axis.

3.3. Fatigue cracking behavior in the crystals containing type III GB

For $[\bar{4}1520]/[18\bar{2}7]$ copper bicrystal, there exists a coplanar slip system between the two component grains, which is similar to that in the columnar crystals. It is expected that the Σ19b GB will be also intrinsically strong resisting intergranular cracking as the low-angle GBs. Cyclic deformation was applied on the bicrystal in the applied axial plastic strain range of 1.5×10^{-4}–2.13×10^{-3}. It is found that all the bicrystal specimens exhibit a cyclic saturation

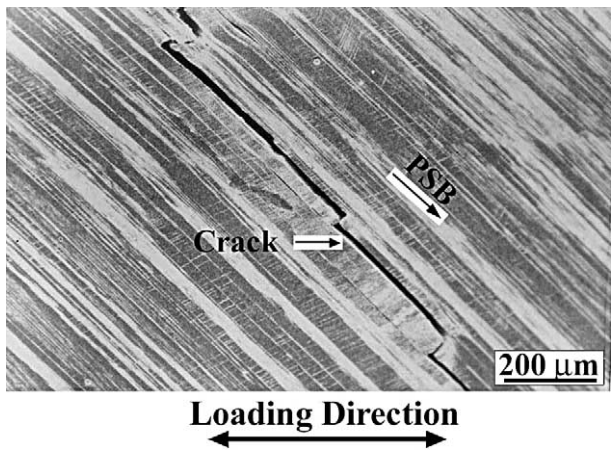

Fig. 10. Fatigue cracking along the PSB in columnar copper crystals containing low-angle GBs.

behavior with nearly the same axis stress of 61.6–63.5 MPa [37]. This result indicates that the cyclic stress–strain response of the $[\bar{4}1520]/[18\bar{2}7]$ bicrystal is also similar to copper single crystals oriented for single-slip [47–49] or the columnar crystals. If taking the Schmid factors (Ω_{G1} = 0.47 and Ω_{G2} = 0.49) of the two grains into account, the saturation resolved shear stresses τ_{G1} and τ_{G2} applied on the primary slip system of the two grains will be in the range of 28.9–29.8 MPa and 30.2–31.1 MPa, respectively, which is approximately equal to the saturation resolved shear stress (28–30 MPa) of the copper single crystal oriented for single-slip. Therefore, it can be concluded that the large-angle Σ19b GB do not produce an obvious strengthening effect on the cyclic stress-strain response of the $[\bar{4}1520]/[18\bar{2}7]$ bicrystal. After cyclic deformation, it is observed that the common primary slip bands are activated on the whole surfaces of the two crystals, including the vicinity of GB. Fig. 11(a) and (b) give typical slip morphologies near the GB on the two surfaces of the bicrystal specimen. It is clear that all the slip bands have a good one-to-one relationship across GB, and no secondary slip bands can be seen. This indicates that the common primary slip bands had transferred through the Σ19b GB without interruption during cyclic deformation, which should be attributed to its special crystallographic relationship of the bicrystal, as shown in Fig. 4. The present results

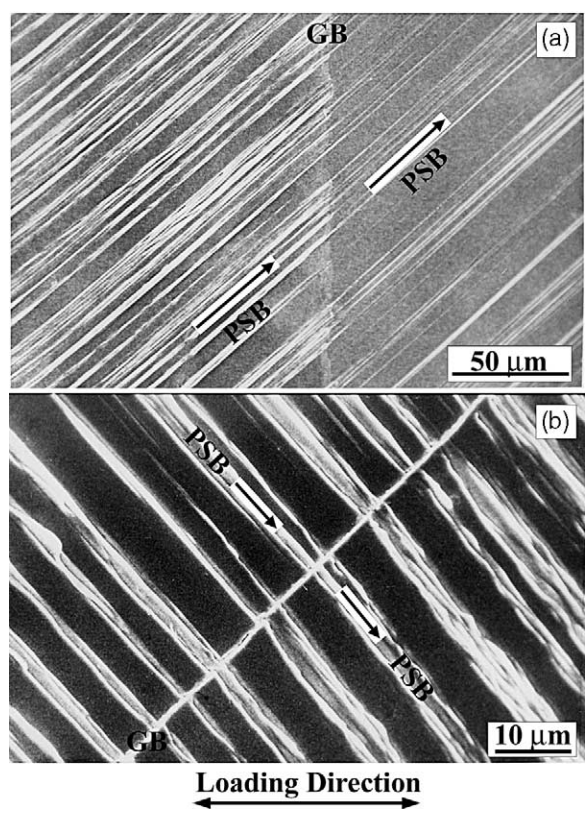

Fig. 11. Surface slip morphologies of the $[\bar{4}1520]/[18\bar{2}7]$ copper bicrystal on (a) the top surface and (b) lateral surface of the bicrystal specimen in Fig. 4(a).

shed light on the similar effect of the Σ19b GB on the stress–strain response and the transmission of PSB across the GB as to the low-angle GBs in the columnar crystals.

When cyclic deformation continues to apply on the bicrystal specimens, however, fatigue crack always initiates at the GB at first, as shown in Fig. 12(a). Beside intergranular fatigue crack, PSBs still have a one-to-one relationship and secondary slip bands are not activated. So the effect of secondary slip bands on the GB cracking can be excluded. With further cyclic deformation, the intergranular fatigue crack gradually propagates along the GB, finally leading to intergranular fatigue fracture along the whole GB, as shown in Fig. 12(b). The present results prove that although surface slip feature of the bicrystal is close to those of a fatigued copper single crystal or columnar crystals containing low-angle GBs, and the GB do not affect the continuity of surface PSBs, eventually fatigue cracking along the GB is still inevitable. Therefore, intergranular fatigue cracking characteristics of the [41520]/[18$\bar{2}$7] bicrystal is similar to the large-angle type I GBs, but is contrary to the low-angle GBs. Although there are similar effects of the Σ19b GB and the low-angle GBs on the stress–strain response and slip morphologies, the fatigue cracking mechanism displays quite different features between them, which is an interesting phenomenon and will be further revealed and discussed in the next section through the observations of dislocations near the GBs.

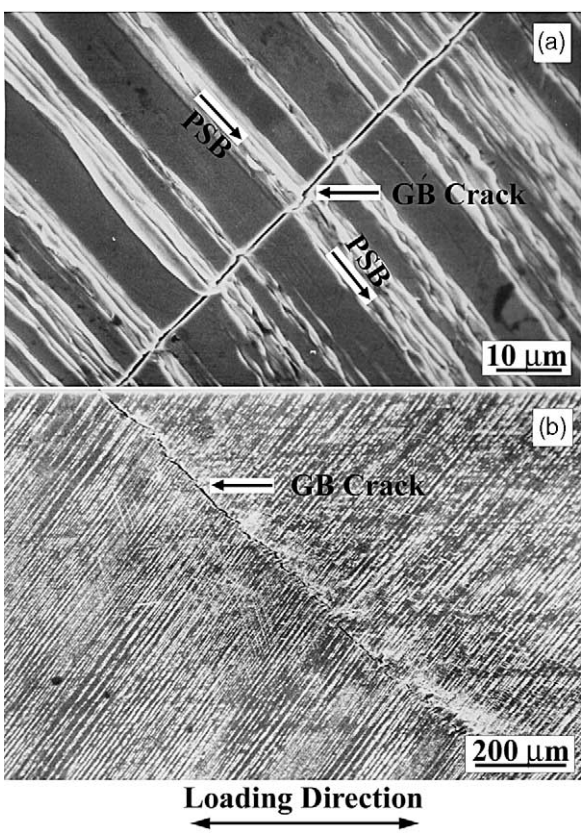

Fig. 12. Fatigue cracking along the Σ19b GB in the [$\bar{4}$1520]/[18$\bar{2}$7] copper bicrystal.

4. Discussion

For f.c.c. metals, it has been recognized that typical fatigue cracking mechanisms are either along PSBs or along GBs or both of them in single or polycrystalline materials [53–60]. Up to now, the widely accepted models for the two typical fatigue cracking are extrusion-intrusion mechanism [61–63] and PSB-GB (or piling-up of dislocations) mechanism [64–67]. Both the models are based on the movements of dislocations in fatigued crystals, therefore, it is necessary to further observe the dislocation arrangements near the GBs for better understanding the difference in fatigue cracking mechanisms along the three types of GBs. Since SEM-ECC technique provides a convenient and applicable way to obtain the dislocation arrangements on a large area and some special sites, all the fatigued specimens have been observed especially near the GBs. Fig. 13(a) shows a typical dislocation arrangements near a large-angle GB perpendicular to the stress axis. It can be seen that some white bands should correspond to PSBs and they can reach GB. When PSBs are close to the GB, their end becomes sharp and irregular. PSBs can also produce certain effect on the adjacent grain, but cannot pass through GB. The dislocation observation further demonstrates that PSBs can not transfer through a large-angle GB, which is consistent with the surface observations (see Fig. 5(a)). When the large-angle GB is parallel to the stress axis, it is found that all the PSBs become irregular

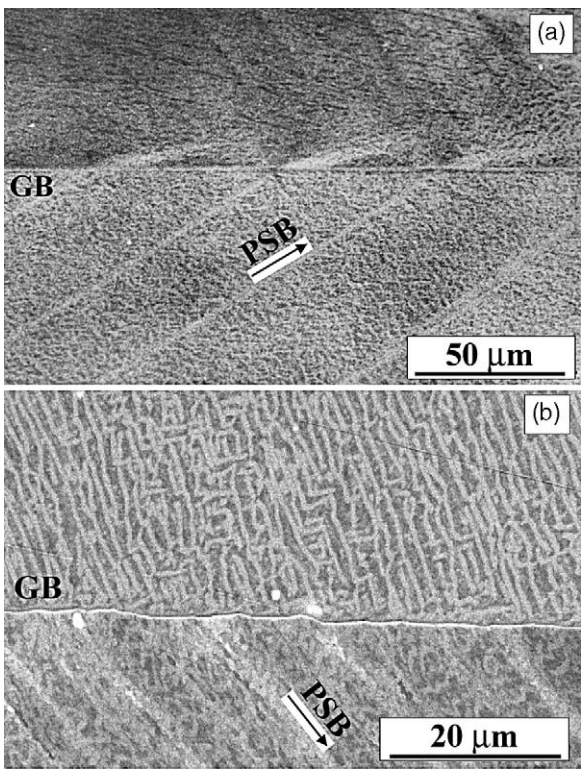

Fig. 13. Dislocation arrangements near the large-angle GB. (a) $[\bar{5}913]\perp[\bar{5}79]$ copper bicrystal with a perpendicular GB: (b) $[\bar{4}916]//[\bar{4}927]$ copper bicrystal with a parallel GB.

near the GB due to the serious plastic strain incompatibility, as shown in Fig. 13(b). In the upper grain, no PSBs can be observed and a labyrinth structure appears in the GBAZ due to the interactions of primary and secondary slip bands (see Fig. 7). From the observations in the vicinity of the large-angle GBs, it should be concluded that the dislocation arrangements beside the type I GB are discontinuous, which can be attributed to the difference in orientations of the adjacent grains and the blocking effect of GB on slip bands. Even the dislocation arrangements are observed by TEM technique, Hu and Wang [38,68] still found the similar phenomenon in $[\bar{1}35]//[\bar{1}35]$ and $[\bar{2}35]//[\bar{2}35]$ copper bicrystals with a parallel GB and a $[\bar{3}45]/[\bar{1}17]$ copper bicrystal with a perpendicular GB. Previously, some investigators proposed some criteria to predict the transmission of dislocations (or slip bands) across large-angle GBs in the crystals subjected to unaxial deformation [69–72]. They found that some dislocations could transfer through a GB under some favorable conditions. But in our observations, the dislocations within PSBs cannot pass all the large-angle GBs, indicating that the transmission conditions of dislocations across a large-angle GB under cyclic loading should be more critical than that under unaxial loading.

Since piling-up of dislocations at large-angle GBs has been widely observed and accepted in fatigued polycrystals, it is natural that the crystallographic relationship between GB and slip systems of the two neighboring grains can be illustrated as in Fig. 14. The activated PSBs can reach the GB, but cannot pass through it because there is no a coplanar slip system. It has been well known that most plastic strains are carried by PSBs during cyclic deformation of f.c.c. metals [15,16]. PSB may become a carrier and channel transporting residual dislocations and vacancies from the interior of grains into GBs. As the residual dislocations and vacancies piled at a large-angle GB are accumulated to be high enough in density, intergranular cracking along GB will occur under external cyclic stress. Consequently, it can be concluded that the essence of intergranular fatigue cracking should be attributed to the reversal interactions of PSBs with GB, or the accumulation of dislocations and vacancies at GB. In other words, the PSB-GB mechanism will dominate the intergranular fatigue

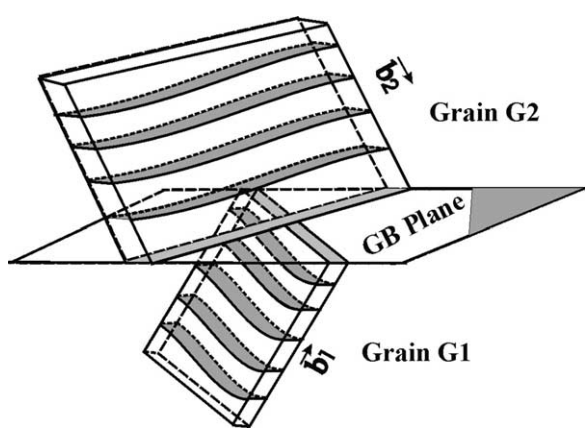

Fig. 14. Illustration of the interactions of the adjacent slip planes with a large-angle GB.

cracking of all the bicrystals with a large-angel GB. In the present investigation, we made the GBs have different angle with respect to the stress axis, however, fatigue cracking always took place along the GB at first, indicating that fatigue cracking is not affected by the interaction angle between GB plane and the stress axis. From the common crystallographic relationship between the GB and the slip systems in Fig. 14, it is natural that the interaction angle cannot change the essence of piling-up of dislocations at the GB. The only case is that the processes of intergranular fatigue cracking become relatively difficult when the GB plane is parallel to the stress axis. Therefore, regardless of the interaction angle between the GB plane and the stress axis, all type I GBs are the preferential sites for the nucleation of fatigue crack, which can be attributed to the piling-up of dislocations at the GBs.

Nowadays, the dislocation arrangements near low-angle GBs under cyclic loading are paid little attention. In the present investigations, SEM-ECC technique has clearly revealed the dislocation patterns near low-angle GBs, as shown in Fig. 15(a), ladder-like PSBs transfer through a low-angle GB continuously. The dislocation arrangement near low-angle GB is consistent with the surface slip morphologies in Fig. 9. To further verify the continuity of dislocation arrangements near low-angle GBs, a more direct method is to observe the dislocation arrangements on the common slip planes. The observation results show that the dislocation patterns near low-angle GB are still continuous, as shown in Fig. 15(b). Since the slip direction of a PSB is perpendicular to the dislocation walls, as indicated by the arrows, the slip directions of the two neighboring grains should be nearly the same. The present observation gives a more powerful evidence that both ladder-like PSBs (see Fig. 15(a)) and parallel dislocation walls (see Fig. 15(b)) are continuous across the low-angle GB. From the observations in Fig. 9 and Fig. 15, it can be concluded that cyclic stress–strain response, surface slip morphology and dislocations are not affected by low-angle GBs during cyclic deformation. Therefore, columnar crystals can be regarded as a single crystal; furthermore, its fatigue cracking mechanism can be in analogy with the single crystals. It has been known that the irreversibility of

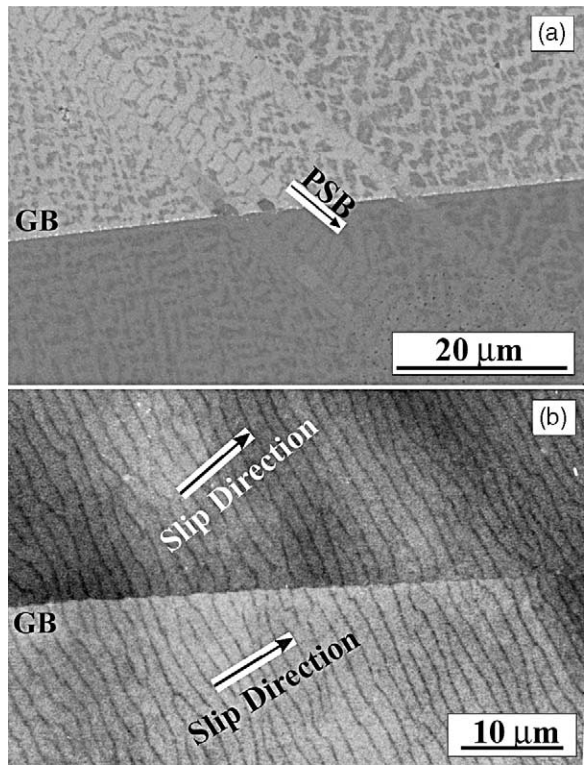

Fig. 15. Dislocation arrangements near the low-angle GB on the surface (a) and on the common primary slip plane (b) in the columnar crystals.

slip within PSBs results in the roughness on the crystal surfaces, which manifests itself in the form of the extrusions and intrusions at the PSB-matrix interfaces. The interfaces between PSBs and matrix are the preferential sites for the nucleation of fatigue cracks in copper single crystals [51,53–55]. The fatigue cracking mechanism in single crystals has been explained by the surface roughness model based on the dislocation annihilation within PSBs [61], as illustrated in Fig. 16(a). Since low-angle GBs in columnar crystals do not block the transmission of the dislocations within PSBs, the interactions of the dislocation walls within a PSB lamina can be illustrated as in Fig. 16(b). The parallel dislocation walls can be transported from one grain into the adjacent grain freely without piling-up of dislocations at the GB. Therefore, the fatigue cracking mechanism of the columnar crystals will be identical with that of copper single crystals,

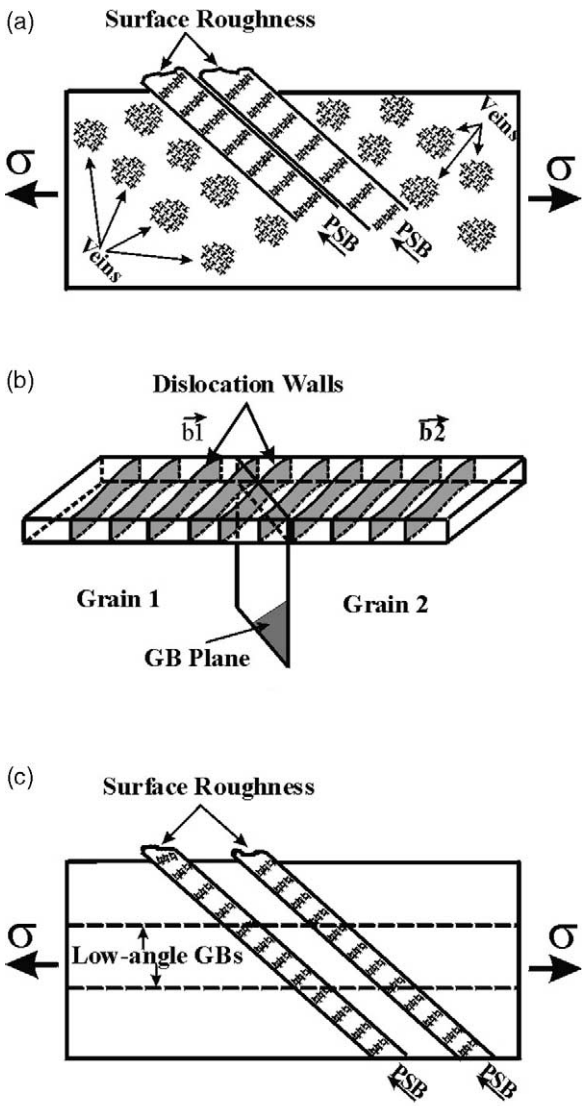

Fig. 16. (a) Illustrations of fatigue cracking along the PSBs in copper single crystals; (b) Illustrations of transmission of dislocation walls across low-angle GBs; (c) Illustrations of fatigue cracking along the PSBs in copper columnar crystal.

which can well explain the PSB cracking in the columnar crystal, as illustrated as in Fig. 16(c).

For $[\bar{4}1520]/[18\bar{2}7]$ bicrystal, SEM-ECC observations also clearly reveal the fatigued dislocation arrangements near the Σ19b GB. Fig. 17(a) shows the typical interaction of Σ19b GB with the dislocations within PSBs on the specimen surface. It can be seen that ladder-like PSBs within one grain

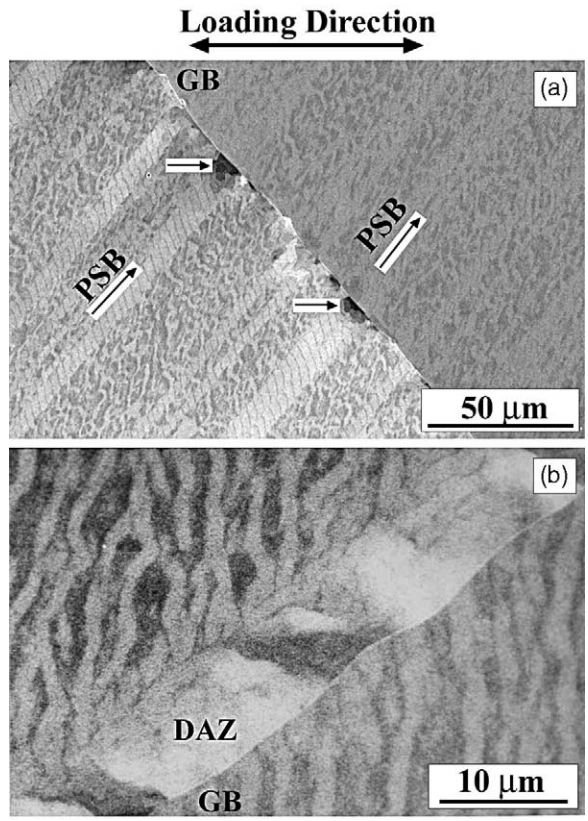

Fig. 17. Dislocation arrangements near the Σ19b GB of the $[\bar{4}1520]/[18\bar{2}7]$ copper bicrystal on the specimen surface (a) and on the common primary slip plane (b).

do not transfer through the GB continuously, but terminate at the GB. However, the dislocation arrangements within PSBs in another grain are not clear due to the difference in the orientation of the two grains. By careful observation, we can see that there seems to exist piling-up of dislocations at the GB, as indicated by the arrows, indicating that the surface slip bands with one-to-one relationship are actually discontinuous. After that, the bicrystal specimen was also cut along the common primary slip plane as in the columnar crystals. In this case, it is found that the dislocation arrangement beside the Σ19b GB is also discontinuous and a dislocation-affected zone (DAZ) appears, as shown in Fig. 17(b). The DAZ is about 10 μm in width and is very similar to the dislocation-free-zone (DFZ) observed by TEM technique in $[\bar{3}45]/[\bar{1}17]$ and

polycrystals [15,38]. The observations above are not consistent with the surface slip bands in Fig. 11, indicating that, actually, ladder-like PSBs cannot completely transfer through the Σ19b GB over the whole specimen despite the two grains in the bicrystal having a coplanar slip system. Therefore, it can be concluded that ladder-like PSBs beside the GB actually are discontinuous, which is acceptable since the slip directions $\mathbf{b}_1$ and $\mathbf{b}_2$ of the two component grains are obviously different, as shown in Fig. 4.

From the dislocation observations, the difference in the fatigue cracking mechanism between the Σ19b GB and the low-angle GBs can be explained by the differences in crystallographic features. As seen in Fig. 4, the primary slip planes of the two component grains are coplanar, whereas, the slip directions $\mathbf{b}_1$ and $\mathbf{b}_2$ have a large angle of 13.8°. Based on the surface slip morphology and dislocation arrangements near the Σ19b GB, the interactions of PSBs with the Σ19b GB can be schematically illustrated in Fig. 18(a) and (b). During cyclic deformation of the bicrystal, the PSBs in the two component grains will impinge at the GB. If the Burgers Vectors $\mathbf{b}_1$ and $\mathbf{b}_2$ of the two PSBs are identical, the dislocations carried by each PSB should easily transfer through the Σ19b GB and move into the adjacent grains, as in the columnar crystals containing low-angle GBs. Because there is an angle of 13.8° between the slip directions $\mathbf{b}_1$ and $\mathbf{b}_2$, actually the dislocations carried by PSBs cannot fully transfer through the Σ19b GB, which has been proved by the observation in Fig. 17. With further cyclic deformation, parts of dislocations carried by PSBs will terminate at the GB, leading to the pilling-up of dislocations. The DAZ near the Σ19b GB in this bicrystal should be direct evidence for the piling-up of dislocations. On the other hand, since the Schmid factors of the secondary slip systems are 0.46 and 0.40, respectively for grains G2 and G1, besides the primary slip system, the secondary slip system may also move the piled dislocation to the neighboring grains. However, the secondary slip system of the two grains were not observed even the intergranular fatigue crack had nucleated, as shown in Fig. 12. It indicates that the effect of the secondary slip system on the GB cracking can be excluded. Therefore, the intergranular fatigue cracking mechanism of the special $[\bar{4}1520]/[18\bar{2}7]$ bicrystal can be still attributed to the piling-up mechanism of dislocations, which is in essence consistent with the damage mechanism of the large-angle Type I GBs.

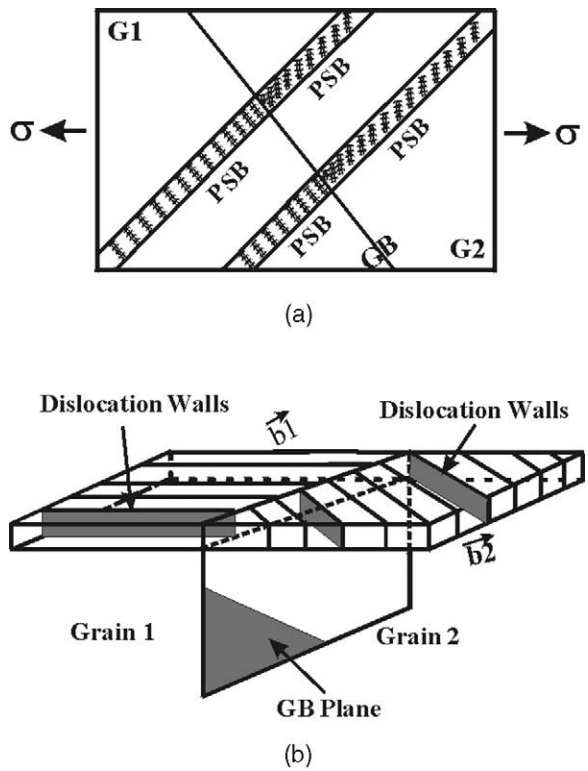

Fig. 18. (a) Illustrations of the interactions of the surface PSBs with the Σ19b GB; (b) Illustrations of the interactions of the dislocation walls with the Σ19b GB on the common primary slip plane in the $[\bar{4}1520]/[18\bar{2}7]$ copper bicrystal.

Based on the results and discussion above, it is apparent that the fatigue damage of the f.c.c. crystals always originates from PSBs or GBs. In essence, the activation of a PSB should correspond to the onset of the micro-damage induced by cyclic deformation. However, the final nucleation of a fatigue crack will depend on the movement processes of the dislocations carried by PSBs. When the dislocations within PSB move from the interior of a grain, they will be transported into the crystal surface if there is no blocking effect of GB in the path of the dislocations. In this situation, the PSB cracking mechanism will dominate the fatigue damage processes and fatigue crack in general

originates from the surface roughness. But in most cases, the dislocations carried by PSBs will always meet a GB, so they will face two choices: (1) fully transmission through the GB; (2) blocking and piling-up at the GB. From our observations, it has been confirmed that only those low-angle GBs can be fully transferred through by the dislocations. Therefore, the dislocations can be moved into the adjacent grains, furthermore reach the surface, and lead to the PSB cracking as shown in Fig. 9, Fig. 10 and Fig. 15. Although some investigators had given some criterions for the transmission of dislocation across a GB under unaxial loading, however, the transmission of dislocations across a large-angle GB is rarely difficult. Even for the special $[\bar{4}1520]/[18\bar{2}7]$ copper bicrystal with a coplanar slip system, the piling-up of dislocations is also observed near the GB, as shown in Fig. 17. It indicates that the piling-up of dislocations near a large-angle GB is a common phenomenon, which will be responsible for the nucleation of GB fatigue crack. Probably, in some special conditions, such as the criteria in the literature [69–72], some dislocations might transfer through a large-angle GB under unaxial loading. However, it should be pointed out that the interactions of dislocations with a GB are very complicated under cyclic loading. Even partial dislocation is kept at GB, the accumulation of the residual dislocations can contribute to the piling-up of dislocations at the GB, and the nucleation of intergranular fatigue cracking. From this viewpoint, therefore, the interactions of PSBs with GBs will strongly affect the fatigue cracking mechanism of f.c.c. metals. According to the GBCD model, some special GBs might exist, which are insensitive to cracking under unaxial loading, such as the GBs with a low value or good match at the boundary. But the adjacent PSBs are, in general, not coplanar beside the GB. For example, $[\bar{4}1520]/[18\bar{2}7]$ bicrystal has a coplanar slip system under the present stress condition. But if the $[\bar{4}1520]/[18\bar{2}7]$ bicrystal is deformed by other stress axis, the primary slip systems of the two component grains will be changed. Although the GB is still Σ19b in type, whereas, the activated PSBs will not be coplanar. Therefore, the intergranular fatigue cracking mechanism of the $[\bar{4}1520]/[18\bar{2}7]$ bicrystal will be similar to those of the bicrystals with a large-angle type I GB. The similar situation should take place in the bicrystals containing the Σ3, Σ5, Σ7, Σ9 GBs and so on. Therefore, the GB structure itself cannot dominate the fatigue cracking mechanism and the interactions of PSBs with GBs should be more important for fatigue crack nucleation. However, for the low-angle GBs, all the slip systems beside the GBs have a coplanar relationship, independent of the stress axis, which results in the non-cracking behavior of the low-angle GBs.

Since intergranular fatigue cracking is attributed to the impingement of PSB to GBs and piling-up of dislocations, we can design other special bicrystals, which are not satisfied with the conditions of piling-up of dislocations at the GB. Furthermore, the intergranular fatigue cracking mechanism can be well understood. One of the ideas is to avoid the impingement of PSBs to GB. According to the principle, the unique case is that both primary slip planes of the two component grains are parallel to the GB plane in a bicrystal with a tilting GB, as illustrated in Fig. 19(a). Meanwhile, it should make the two component crystals orient for typical single slip so that the impingement of the secondary slip bands to the GB can be avoided during cyclic deformation. In this case, the activated primary slip bands will not impinge on the GB, however, the fatigue crack mechanism in such a bicrystal is still a maze. The second way is to make the slip planes

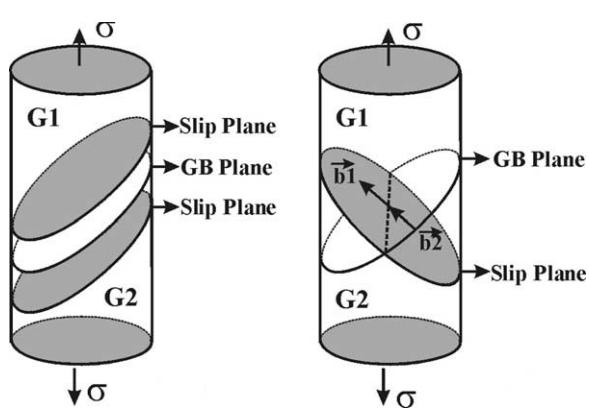

Fig. 19. Illustrations of crystallographic relationships in two special bicrystals: (a) both of the primary slip planes of two component crystals in the bicrystal are parallel to the GB plane; (b) the primary slip systems of two component crystals are coplanar and have the identical slip directions.

of two component grains still coplanar, as in the $[\bar{4}1520]/[18\bar{2}7]$ bicrystal. But the slip directions of the two crystals are also the same as illustrated in Fig.19(b). Since the $[\bar{4}1520]/[18\bar{2}7]$ bicrystal is created by rotating 46.2° from one component crystal around the common rotation [111] axes, the new designed bicrystal can be produced by rotating 60° around the common axis of [111] axes, accordingly a $\Sigma 3$ GB will form between the two crystals. As a result, the GB in the specially designed bicrystal should belong to the second type with a coplanar slip system and identical slip directions, whereas, it is a large-angle one. The identical slip directions between the two component crystals might result in the full passing through of the dislocations across the GB and the piling-up of dislocations at the GB will disappear during cyclic deformation. Furthermore a fatigue crack might nucleate along the PSBs and the specially designed $\Sigma 3$ GB will become intrinsically strong to fatigue cracking as in the low-angle GBs. However, the experimental work should be further carried out on the two presumptions.

5. Summary

From the experimental results above, the following conclusions can be drawn:

1. For all the large-angle GBs in copper bicrystals, fatigue cracks always prefer to nucleate at the GBs, rather than along PSBs. The GB cracking is independent of the interaction angle between the GB plane and the stress axis. The intergranular fatigue cracking can be well explained by the PSB-GB damage (or piling-up of dislocations) mechanism.
2. For the columnar copper crystals containing low-angle GBs, fatigue cracks preferentially initiate along PSBs, rather than along low-angle GBs. The PSB cracking mechanism in essence is identical with that in fatigued copper single crystals. The main reason for the non-cracking behavior of the low-angle GBs is that the dislocations carried by PSBs can be fully transported from one grain to adjacent grain through their coplanar slip system. In other words, the low-angle GBs do not block the transmission of dislocations carried by PSBs, therefore, no piling-up of dislocations exists at the low-angle GB.
3. For a special $[\bar{4}1520]/[18\bar{2}7]$ copper bicrystal with a coplanar slip system, surface PSBs are continuous across the $\Sigma 19b$ GB after cyclic deformation. However, the GB is still the preferential site for the nucleation of fatigue crack even though the two component crystals have a coplanar slip system. The fatigue cracking mechanism can be attributed to the difference in the slip directions of the adjacent grains. Therefore, the dislocations carried by PSBs cannot be fully moved into the adjacent grain through the coplanar slip. The partial dislocations are kept at the GB and form a dislocation-affected-zone (DAZ). The DAZ should be direct evidence for the piling-up of dislocations at the $\Sigma 19b$ GB. Essentially, the fatigue cracking mechanism of the $\Sigma 19b$ GB is identical with all the large-angle type I GBs, i.e. pilling-up mechanism.
4. It is suggested that intergranular fatigue cracking depends strongly on the interactions of PSBs with GBs, rather than the GB structure itself. The nucleation of fatigue cracks along a PSB or a GB is a competitive process, depending on the movement processes of dislocations carried by PSB. The fatigue damage of the ductile f.c.c. crystals originates from the activation of dislocations carried by slip bands. When the dislocations can be freely transported to the surface by slip bands, the gradual surface toughness will become the origin of a fatigue crack, in most cases, resulting in PSB cracking. When dislocations carried by PSBs cannot transfer through a GB, they will pile-up at the GB, furthermore result in the intergranular fatigue cracking due to the accumulation of the residual dislocations.

Acknowledgements

This work was financially supported by the Special Funding for the National 100 Excellent Ph. D Thesis provided by Chinese Academy of Sciences. The authors are grateful to Prof. C. Holste, Prof. C. Blochwitz and Dr. A. Schwab at Technical Uni-

versity of Dresden for their stimulating discussions. Thanks are also due to H. H. Su for his assistance in the careful observations by using the SEC-ECC technique. One of the authors (Zhang, Z. F.) also wishes to acknowledge the Alexander von Humboldt (AvH) Foundation for providing a postdoctoral fellowship.

References

[1] Kung H, Foecke T. MRS Bull 1999;24:14–5.
[2] Weertman JR, Farkas D, Hemker K, Kung H, Mayo M, Mitra R et al. MRS Bull 1999;24:44–50.
[3] Gleiter H. Acta Mater 2000;48:1–29.
[4] Lu L, Sui ML, Lu K. Adv. Eng. Mater 2001;3:663–7.
[5] Pander V. Acta Mater 1997;45:1459–80.
[6] Watanabe T, Tsurekawa S. Acta Mater 1999;47:1459–80.
[7] Briant CL. Mater. Sci. Tech 2001;17:1317–23.
[8] Gourgues AF. Mater. Sci. Tech 2002;18:119–33.
[9] Watanabe T. Res. Mech 1984;11:47–58.
[10] Watanabe T, Fujii H, Oikawa H, Arai KI. Acta Metall 1989;37:47–56.
[11] Aust KT, Erb U, Palumbo G. Mater. Sci. Engng. 1994;A176:329–36.
[12] Kobayashi S, Yoshimura T, Tsurekawa S, Watanabe T. Mater. Sci. Forum 1999;304-306:591–602.
[13] Pan Y, Adams BL, Olson T, Panayotou N. Acta Mater 1996;44:4685–95.
[14] Adams BL, Zhao JW, Ohara D. Acta Metall. Mater 1990;38:953–66.
[15] Luoh T, Chang CP. Acta Mater 1996;44:2683–95.
[16] Zauter R, Petry F, Bayerlein M, Sommer C, Christ H-J, Mughrabi H. Phil. Mag. 1992;A66:425–36.
[17] Ahmed J, Wilkinson AJ, Roberts SG. Phil. Mag. Lett. 1997;A76:237–45.
[18] Melisova D, Weiss B, Stickler R. Scripta Mater 1997;36:1601–5.
[19] Alus H, Bussiba A, Katz Y, Gerberich WW. Scripta Mater 1998;39:1669–74.
[20] Schwab A, Holste C. Acta Mater 2002;50:289–303.
[21] Zhang ZF, Wang ZG. Phil. Mag. Lett. 1998;A78:105–13.
[22] Jia WP, Li SX, Wang ZG, Li XW, Li GY. Acta Mater 1999;47:2165–76.
[23] Gong B, Wang ZR, Chen DL, Wang ZG. Scripta Mater 1997;37:1605–10.
[24] Zhang ZF, Wang ZG, Sun ZM. Acta Mater 2001;49:2875–86.
[25] Wilkinson AJ, Henderson MB, Martin JW. Phil. Mag. Lett 1996;74:145–51.
[26] Huang HJ, Ho NJ. Mater. Sci. Engng. 2001;A298:251–61.
[27] Zhang ZF, Wang ZG. Mater. Sci. Engng. 1998;A255:148–53.
[28] Zhang ZF, Wang ZG, Hu YM. Mater. Sci. Engng. 1999;A269:136–41.
[29] Zhang ZF, Wang ZG. Phil. Mag. 1999;79A:741–52.
[30] Zhang ZF, Wang ZG, unpublished work.
[31] Zhang ZF, Wang ZG. Acta Mater 1998;46:5063–72.
[32] Zhang ZF, Wang ZG, Hu YM. Mater. Sci. Engng. 1999;A272:412–9.
[33] Zhang ZF, Wang ZG, Hu YM. Mater. Sci. Tech 2000;16:157–62.
[34] Zhang ZF, Wang ZG, unpublished work.
[35] Zhang ZF, Wang ZG, Li SX. Fatigue Fract. Engng. Mater. Struct 1998;21:1307–16.
[36] Zhang ZF, Li XW, Su HH, Wang ZG. J. Mater. Sci. Tech 1998;14:211–4.
[37] Zhang ZF, Wang ZG. Phil. Mag. 2001;81A:399–415.
[38] Hu YM, Wang ZG. Acta Mater 1997;45:2655–70.
[39] Hu YM, Wang ZG. Int. J. Fatigue 1998;20:463–8.
[40] Peralta P, Laird C. Acta Mater 1997;45:3029–46.
[41] Peralta P, Laird C. Acta Mater 1998;46:2001–20.
[42] Hashimoto S, Vinogradov A. Interface Science 1996;4:347–55.
[43] Shodja HM, Hirose Y, Mura T. J. Appl. Mech. Trans., ASME 1996;63:788–95.
[44] Hu YM, Wang ZG, Li GY. Mater. Sci. Engng. 1996;A208:260–9.
[45] Hauser JJ, Chalmers B. Acta Metall 1961;9:802–18.
[46] Hirth J-P. Metall. Trans 1972;3:3047–67.
[47] Chuang Y-D, Margolin H. Metall. Trans. 1973;A4:1905–17.
[48] Paidar V, Pal-val PP, Kadeckova S. Acta. Metall 1986;34:2277–89.
[49] Mughrabi H. Mater. Sci. Engng 1978;33:207–23.
[50] Chen AS, Laird C. Mater. Sci. Engng 1981;51:111–21.
[51] Basinski ZS, Basinski SJ. Prog. Mater. Sci 1989;36:89–148.
[52] Kehagias Th, Komninou Ph, Dimitrakopulos GP. Scripta Metall. Mater 1995;33:1883–8.
[53] Basinski ZS, Basinski SJ. Scripta Metall 1984;18:851–6.
[54] Hunsche A, Neumann P. Acta Metall 1986;34:207–17.
[55] Ma BT, Laird C. Acta Metall 1989;37:325–36.
[56] Figueroa JC, Laird C. Mater. Sci. Engng 1983;60:45–58.
[57] Lim LC. Acta. Metall 1987;35:1653–62.
[58] Huang HL, Ho NJ. Mater. Sci. Engng. 2000;A293:7–14.
[59] Tvergaard V, Wei Y, Hutchinson JW. Eur. J. Mech. A/Solids 2001;20:731–8.
[60] Blochwitz C, Tirschler W, Mater. Sci. Engng., 2002, in press.
[61] Essmann U, Gosele U, Mughrabi H. Phil. Mag. 1981;A44:405–26.
[62] Differt K, Essmann U, Mughrabi H. Phil. Mag. 1986;A54:237–58.
[63] Repetto EA, Oritz M. Acta Metall 1997;45:2577–95.
[64] Christ HJ. Mater. Sci. Engng. 1989;117:L25–9.
[65] Liu W, Bayerlein M, Mughrabi H, Day A, Quested PN. Acta Metall. Mater 1992;40:1763–71.
[66] Burmeister H-J, Tichter R. Acta Mater 1997;45:709–14.
[67] Lin TH, Wong KKF, Teng NJ, Lin SR. Mater. Sci. Engng. 1998;A246:169–79.

[68] Hu YM, Wang ZG. Mater. Sci. Engng. 1997;A234-236:98–101.
[69] Davis KG, Teghtsoonian E, Lu A. Acta Metall 1966;14:1677–84.
[70] Baunford T, Hardiman AB, Shen Z, Clark WAT, Wagoner RH. Scripta Metall 1982;20:253–8.
[71] Shen Z, Wagoner RH, Clark WAT. Acta Metall 1988;36:3231–42.
[72] Lee TC, Robertson IM, Birnbaum HK. Scripta Metall 1989;23:799–803.